Liquid Crystals
Publication details, including instructions for authors and subscription information:
http://www.informaworld.com/smpp/title~content=t713926090

Material characteristics of an active matrix LCD based upon chiral smectics

Toshiaki Nonaka; Ji Li; Ayako Ogawa; Barbara Hornung; Wolfgang Schmidt; Rainer Wingen; Hans-Rolf Dubal

Online publication date: 06 August 2010

To cite this Article Nonaka, Toshiaki , Li, Ji , Ogawa, Ayako , Hornung, Barbara , Schmidt, Wolfgang , Wingen, Rainer and Dubal, Hans-Rolf(1999) 'Material characteristics of an active matrix LCD based upon chiral smectics', Liquid Crystals, 26: 11, 1599 — 1602
To link to this Article: DOI: 10.1080/026782999203580
URL: http://dx.doi.org/10.1080/026782999203580

LIQUID CRYSTALS, 1999, VOL. 26, NO. 11, 1599–1602

Material characteristics of an active matrix LCD based upon chiral smectics

TOSHIAKI NONAKA, JI LI, AYAKO OGAWA
Clariant Japan K.K, NBD Laboratory/FLC group, 3810 Chihama, Daito-cho, Ogasa-gun, Shizuoka 437-1496, Japan

BARBARA HORNUNG, WOLFGANG SCHMIDT, RAINER WINGEN and HANS-ROLF DÜBAL*
Clariant GmbH, Projekt FLC, Industriepark Höchst D 528, D-65926 Frankfurt/Main, Germany

(*Received 22 January 1999; in final form 7 May 1999; accepted 22 May 1999*)

We describe the material properties of a fast switching active matrix ferroelectric liquid crystal mode. The mode relies on a monostable monodomain having a high transmission and full grey scale capability. Experimental data are compared with the results of switching model calculations and the switching mechanism is discussed. The mode is suitable for video and multimedia application and compatible with conventional amorphous silicon thin film transistors due to the small value of the spontaneous polarization.

1. Introduction

The application of the active matrix liquid crystal display (AM-LCD) for multimedia monitors requires liquid crystal material that provides high contrast, high brightness, high speed, full colour representation and a wide viewing angle. In addition, a low driving voltage, ideally below 3.3 V, is requested. Today's LCDs can only partly fulfill these demands. We mention here the active matrix (AM) technologies utilizing nematics which are known as AM-TN, AM-IPS, AM-VA [1], all having a comparatively low speed and requiring driving voltages of 5 V or more in order to obtain high luminance. On the other hand, several groups have developed chiral smectic displays such as the bistable SSFLC [2] both in normal [3, 4] and inverse [5, 6] mode. Further work has also been done in the area of silicon backplane FLC displays [7, 8] and flexible polymeric and low molecular mass FLC displays [9, 10].

There are two major advantages of FLC displays: the 'pixel speed' is easily 100 or even 1000 times faster than for nematics and secondly, due to the bistability, the resolution of such displays is not limited by the material. However, passive matrix FLC displays are limited by certain trade-off relationships: the higher the number of scanning lines, the higher is the frame addressing time and thus the speed of a display is always in competition with its resolution. Nevertheless, it is stressed that far from a complete register of performance criteria in FLC technology has been drawn up and there is certainly space for significant further improvements.

With respect to the trade-offs of passive matrix FLC displays, several authors have suggested combining the active matrix with FLC. The first approach was made by Hartmann [11] in the 80s utilizing the charge-controlled bistability of a quasi-bookshelf FLC with MOS-FET technology. Recently, Takatoh *et al.* [12] demonstrated an AM display based upon chiral smectics using a very high $\mathbf{P}_S$ material driven with an active matrix with polycrystalline silicon-TFT. Nito *et al.* [13] also suggested a monostable AM-FLC with much lower $\mathbf{P}_S$, however, with the disadvantage of a stripey FLC texture which is not suitable for high contrast displays without further improvements; Furue *et al.* [14] suggested a polymer-stabilized SSFLCD with a FELIX® mixture with a moderate $\mathbf{P}_S$ value.

In this paper, we would like to describe material parameters and the switching characteristics of a new AM-FLC mode. The display aspects have been described by Terada *et al.* [15]. In this mode, monodomains with high cone angle are obtained by a d.c. field supported alignment technique, previously described by several authors [16–20]. These domains can be switched at low voltage with rather high speed. Furthermore, a multitude of grey levels is addressable and a wide viewing angle is obtained naturally.

*Author for correspondence.

Journal of Liquid Crystals ISSN 0267-8292 print/ISSN 1366-5855 online
http://www.tandf.co.uk/JNLS/lct.htm
http://www.taylorandfrancis.com/JNLS/lct.htm

2. Experimental

We made test cells from ITO-coated glass, the electrodes being coated with a thin alignment layer based upon LQT-120 (Hitachi Chemicals KK, Japan). The alignment layer is then cured and rubbed, and the cell glasses are assembled for parallel alignment and glued together. An experimental FLC mixture with the phase sequence: smectic C* (SmC*)—cholesteric (N*)—isotropic (I) is filled in by capillary forces.

We obtained a mono-domain alignment by applying a d.c. electric field upon cooling the cell in the temperature range of $T_{SmC^*-N^*} \pm 2°C$, where $T_{SmC^*-N^*}$ is the transition temperature from the cholesteric to the smectic phase; the d.c. field strength was typically $2.5\,V\,\mu m^{-1}$. After this alignment, which has been described before by several authors [16–20], we allowed the cell to cool further to room temperature in order to perform our experiments. Properties of the test mixtures are summarized in table 1.

3. Electro-optical characteristics

First, the transmission of the cell between crossed polarizers in a microscope was measured, while recording the brightness with a photodiode as a function of the voltage applied to the cell. We used monopolar rectangular pulses of 16.7 ms width and varied the voltage amplitude. The result is shown in figure 1.

The T, V curve has a threshold at a very low voltage that depends on the $\mathbf{P}_S$ value and the anchoring forces. The higher the $\mathbf{P}_S$, the lower the threshold for the same anchoring forces. For higher voltages, the transmission increases continuously finally to reach saturation. By matching the cell thickness to the effective birefringence, it is easy to obtain the theoretical limit of the transmission maximum as the effective cone angle can be easily adjusted to 45 degrees.

The switching on and off times, as defined by the 0–90% and 100–10% ($3\,V\,\mu m^{-1}$) transmission times, respectively, are given in table 2. Other than in bistable SSFLC they are not equal, thus reflecting the monostable configuration.

4. Switching mechanism

Figure 2 shows (*a*) the position of the smectic C* cone with respect to the rubbing direction, (*b*) a side view of the expected smectic layer structure and (*c*) a front view of the switching cone indicating the *c*-director and the monostable position, in which the projection of the *n*-director onto the electrode surface is parallel to the rubbing direction.

The second outer position on the switching cone which would be the other stable position in an ordinary SSFLC is de-stabilized due to the fact that a large

Table 1. Properties of the test mixtures used in the experiments.

Mixture	Transition temperature/°C			$\mathbf{P}_S$/nc cm^{-2}
	I–N*	N–SmC*	SmC*–X	
A	71.5–70.3	53.9	– 4	3.5
B	71.5–71.0	53.5	– 4	6.7
C	71.3–70.8	52.9	– 5	13.3

Table 2. On and off switching times, measured at 30°C.

Mixture	τ_{on}/ms	τ_{off}/ms
A	1.8	0.2
B	0.9	0.2
C	0.8	0.3

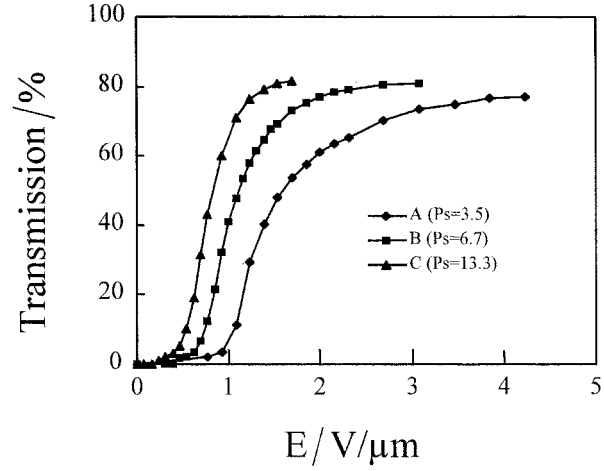

Figure 1. The T, V characteristics for mixtures A, B, C at 30°C. 100% transmission means an empty cell of 1.3 μm thickness between a pair of parallell polarizers.

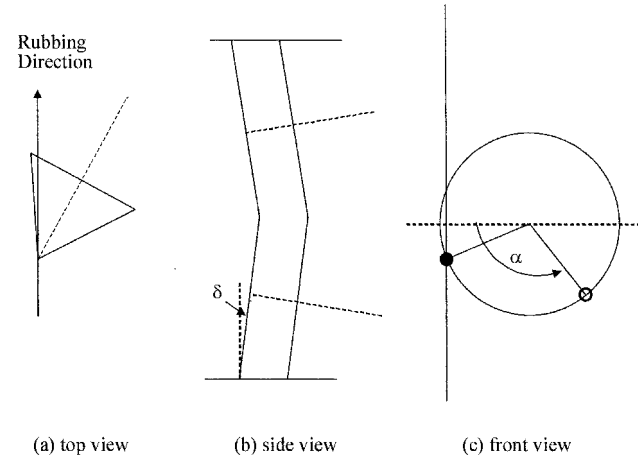

Figure 2. Director configuration: the monostable position is in the rubbing direction and is denoted by the full circle in (*c*); see text for details.

deviation from the rubbing direction leads to an increase of the potential energy.

In a simple form, neglecting layer deformation and volume effects and with no field applied, the free energy density is:

$$G = G_R + G_E \tag{1}$$

where G_R and G_E are the rubbing and elevation energy densities, respectively. The rubbing term G_R has a minimum, if the projection of the n-director towards the electrode surface is parallel to the rubbing direction. The elevation term G_E takes into account the fact that the n-director prefers a horizontal position.

With applied field, we get:

$$G = G_R + G_E + G_D + G_F \tag{2}$$

with:

$$G_D = -\frac{1}{2}\varepsilon_0 \varepsilon \mathbf{E}\mathbf{E} \tag{3}$$

$$G_F = -\mathbf{P}_S \mathbf{E}. \tag{4}$$

Here ε is the dielectric tensor, $\mathbf{E}$ the electric field and $\mathbf{P}_S$ the spontaneous polarization vectors, respectively.

Figure 3 displays the results of such calculations. The free energy density (in $J\,m^{-3}$) is plotted as a function of the α-angle that specifies the position of the c-director; $\alpha = 0°$ means the 9 o'clock and $\alpha = 90°$ is the 6 o'clock position in figure 2 (c). Without applied field, the energy minimum position is nearly, but not exactly, at the $\alpha = 0°$ position. This is due mainly to the fact that the layer leaning angle differs from zero.

Because the monostable position for 0 V falls almost on the cone periphery, the switching by a field opposite to the aligning field occurs gradually, induced by the ferroelectric term in equation (4). The free energy minimum shifts towards higher α-values and gradually accesses the whole range of α-values. This continues until full switching is obtained. For higher fields, some additional contribution of the dielectric term is observed.

A striking feature is the full control of the threshold and saturation voltages by the value of the spontaneous polarization. Thus, the driving voltage can be adjusted to even below 3 V, if desired. Figure 4 displays a comparison of calculated and observed T, V data.

Based upon these considerations, we illustrate the basic switching mechanism in figure 5. Position 1 is the field-free monostable position as discussed above. Upon

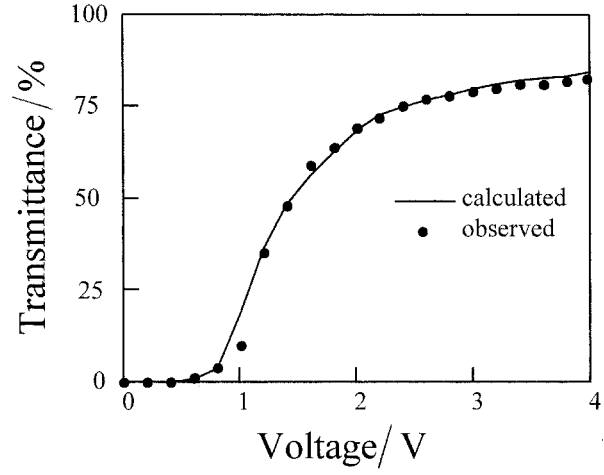

Figure 4. Comparison of experimental and calculated values (T, V) for mixture B: $\mathbf{P}_S = 6.7\,nC\,cm^{-2}$, $\theta = 26°$, $\delta = 12°$, $d = 1.3\,\mu m$, $\Delta n = 0.173$, $\lambda = 600\,nm$, $\varepsilon_1 = \varepsilon_2 = \varepsilon_3 = 3$, maximum rubbing energy density = $130\,J\,m^{-3}$, maximum elevation energy density = $250\,J\,m^{-3}$.

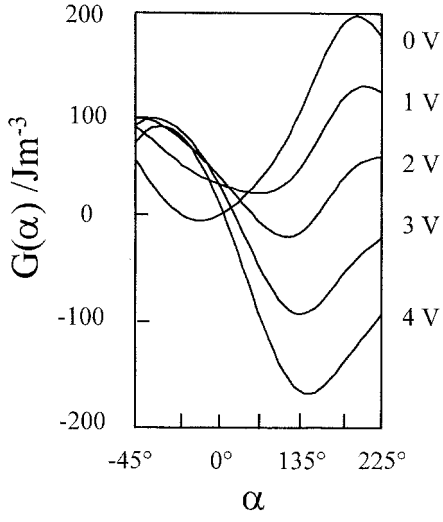

Figure 3. Free energy density as a function of the voltage for a cell thickness of 1.3 μm calculated using equation (2); see also figure 4.

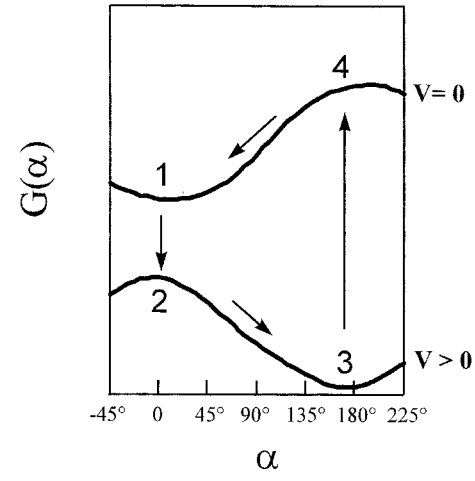

Figure 5. Sketch of the switching cycle. The on-switching is governed by the transition 2→ 3, the off-switching by the relaxation from 4→ 1.

turning on the field, the *c*-director 'drops' to another energy potential curve (position 2) and rotates into the new minimum position 3. After turning off the field, the stabilization effect of $-\mathbf{P}_S\mathbf{E}$ is removed and the *c*-director finds itself in the unstable position 4, from which it relaxes back into position 1.

The dynamics of the transitions $2\rightarrow 3$ and $4\rightarrow 1$ which define the on and off times, respectively, are given by:

$$\gamma\frac{d\alpha}{dt}=\frac{dG}{d\alpha}. \tag{5}$$

Here, γ is the rotational viscosity with respect to the *c*-director. Besides viscosity, the slope $dG/d\alpha$ governs the switching speed. On the other hand, for $2\rightarrow 3$ (τ_{on}) the speed depends on $\mathbf{P}_S$; the τ_{off} relaxation is independent of $\mathbf{P}_S$ and depends only on anchoring forces, as long as monopolar pulses which do not reverse the field are applied.

At this point, we would like to emphasize an important difference from ordinary bistable FLC displays. Whereas the bistable SSFLC has a *dynamic* threshold, as defined by the balance of viscous and ferroelectric (and dielectric) torques, this new mode has a *static* threshold that is defined by the ratio of the ferroelectric and anchoring energies. Thus, no viscosity term enters the threshold voltage, resulting in a *T*, *V* characteristic that is almost independent of temperature. The threshold voltage is roughly proportional to $1/\mathbf{P}_S$ and this explains the peculiar observation that a lower temperature shows a somewhat smaller threshold voltage (but, of course, also a somewhat lower speed).

5. Conclusion

The switching characteristics described here open the opportunity for a novel class of active matrix LCD with high speed, full colour, wide viewing angle, etc. (see Terada *et al.* [15]). For each value of the applied voltage a well defined energy minimum position of the *c*-director is obtained. Thus, by tuning the field, the *c*-director is continuously rotated. In combination with an active matrix, the rotated position is held by a quasi-static electric field. For this reason, we suggest calling this effect 'continuous director rotation' (CDR) and the respective display AM-CDR.

These active matrix displays combine a high performance, full colour image with high speed, low voltage driving and—last but not least—conventional amorphous Si-TFT technology due to the small $\mathbf{P}_S$ value of the FLC material used.

References

[1] Geelhaar, T., 1998, *Liquid crystals for innovative displays*, presented at the BMBF conference, 16 October 1998, St. Augustin, Germany.

[2] Clark, N. A., and Lagerwall, S. T., 1980, *Appl. Phys. Lett.*, **36,** 899; Clark, N. A., and Lagerwall, S. T., 1983, US Patent 4 367 924.

[3] Mitzutani, H., Tsuboyama, A., Hanyu, Y., Okada, S., Terada, M., and Katagiri, K., 1997, presented at the 6th International Conference on Ferroelectric Liquid Crystals, 20–24 July 1997, Brest, France.

[4] Kanbe, J., Inoue, H., Mizutome, A., Hanyu, Y., Katagiri, K., and Yoshihara, S., 1991, *Ferroelectrics*, **114,** 3.

[5] Bradshaw, M. J., Brown, C. V., Haslam, S. D., Hughes, J. R., Graham, A., Jones, J. C., McDonnell, D. G., Katsuse, H., Kawabata, Y., Koden, M., Miyoshi, S., Nonomura, K., Numao, T., Shigeta, M., Sugino, M., Tagawa, A., Gass, P. A., Raynes, E. P., and Towler, M. J., 1997, presented at the SID Conference IDRC, L-16, Toronto, Canada.

[6] Hughes, J. R. and Raynes, E. P., 1993, *Liq. Cryst.*, **13,** 199.

[7] Wand, M. D., 1997, Summary of the 6th International Conference on Ferroelectric Liquid Crystals, 20–24 July 1997, Brest, France, 68; see also http://www.displaytech.com

[8] Surguy, P. W. H., Ayliffe, P. J., Birch, M. J., Bone, M. F., Coulson, I., Crossland, W. A., Hughes, J. R., Ross, P. W., Saunders, F. C., and Towler, M. J., 1991, *Ferroelectrics*, **122,** 63.

[9] Togawa, S., 1996, Electr. Eng., **38,** 79; Yuasa, K., Uchida, S., Sekiya, T., Hashimoto, K., and Kawasaki, K., 1991, *Ferroelectrics*, **122,** 53.

[10] Bürkle, R., Klette, R., Lüder, E., Bunz, R., and Kallfass, T., 1997, *SID Dig.*, **109** (9.4); Bürkle, R., 1998, Dissertation, Stuttgart, Germany, ISBN 3-8265-3423-9.

[11] Hartmann, W. J. A. M., 1989, *IEEE Trans. Electron. Devices*, **36,** 1895.

[12] Takatoh, K., 1997, presented at the 6th International Conference on Ferroelectric Liquid Crystals, 20-24 July 1997, Brest, France; Okumura, H., Akiyama, M., Takatoh, K., and Uematsu, Y., 1998, *SID Dig.*, 1171.

[13] Nito, K., Matsui, E., Miyashita, M., Arakawa, S., and Yasuda, A., 1993, *J. SID*, **1/2,** 163.

[14] Furue, H., Iimura, Y., Hasebe, H., Takatsu, H., and Kobayashi, S., 1998, in Proceedings of *IDW'98*, pp. 209–212.

[15] Terada, M., Togano, T., Asao, Y., Moriyama, T., Nakamura, S., and Iba, J., 1999, presented at the Applied Physics Conference, 28 March 1999, Tokyo, Japan, Abstract No. 28p-V-8.

[16] Nakayama, K., Ozaki, M., and Yoshino, K., 1998, *Jpn. J. appl. Phys.*, **37,** 5379.

[17] Goodby, J. W., 1991, *Properties and structures of ferroelectric liquid crystals,* Ferroelectricity and Related Phenomena series, Vol. 7, edited by G. W. Taylor (Reading: Gordon and Breach Science Publishers), p. 234ff.

[18] Bradshaw, M. J., and Raynes, E. P., 1991, US Patent 5 061 047.

[19] Bradshaw, M. J., and Raynes, E. P., 1990, US Patent 4 969 719.

[20] Patel, J., and Goodby, J. W., 1986, *J. Appl. Phys.*, **59,** 2355.